**Responses to the comments of zhao zhang**

**Article ID:** essd-2026-284

**Title:** NortheastChinaMaizeYield10m: A 10-m Resolution Maize Yield Dataset for Northeast China (2019–2024) Generated via a Mechanistically Interpretable, Label-free Framework

**Authors:** Jingbo Hu, Xin Du, Qiangzi Li, Yuan Zhang, Hongyan Wang, Jiansong Luo, Jingyuan Xu, Yachao Zhao, Zhaoming Zhang, Yong Dong, and Yunqi Shen

Dear Reviewer,

Thank you very much for your thorough review and constructive feedback on our manuscript. We have carefully addressed each comment and suggestion to refine our work, enhance its clarity and strengthen its scientific contribution. The key revisions include:

(1). **Refined the terminology "label-free" to "field-label-free training".** We have consistently replaced this term throughout the manuscript to precisely clarify that our framework is free of real-world in situ yield annotations during model training.

(2). **Strengthened baseline comparisons by incorporating LSTM models.** We implemented LSTM networks under the optimal feature configuration to better justify our architectural choice.

(3). **Enhanced mechanistic interpretability through SHAP analysis.** We conducted SHAP analysis on the optimal GRU model to quantify the contribution of each feature to yield prediction.

(4). **Provided uncertainty layers and bootstrap confidence intervals.** We generated 10-meter resolution uncertainty maps (CV) for 2023 and 2024, which are now released alongside the yield product. Due to the intensive computational workload associated with pixel-wise uncertainty quantification across our large-scale study area (approximately $1.24 \times 10^6$ km²) and the current data download and processing constraints of the Google Earth Engine (GEE) platform, we have currently completed and released the uncertainty layers for 2023 and 2024 as a first priority. The remaining years (2019–2022) are under active production and will be released progressively upon completion. We also conducted bootstrap resampling to report 95% confidence intervals for all deep learning model configurations in Appendix A.

(5). **Added comparison with existing public yield products.** We compared our product with the published "A 10 m maize, rice and soybean yield dataset from 2016 to 2021 in Northeast China" (Teng et al., 2026) through both quantitative and visual assessments.

(6). **Added county-level validation.** We collected official county-level maize yield statistics for 2019–2024 and conducted additional validation at this finer administrative scale.

(7). **Expanded discussion on simulation-to-reality gap and clarified simulation design rationale.** We added dedicated discussion on uncertainties and clarified that our full-factorial design prioritizes physiological state space coverage with quality-controlled samples.

The detailed point-to-point responses are as follows. Texts in **black** are the reviewer's comments; those in **blue** are our responses to the reviewer's comments; and those in ***red and italics*** are the revised texts appeared in the revised manuscript.

I find the general idea of this study quite innovative. In particular, the use of crop-model simulations to generate training samples, combined with remote-sensing time-series data for high-resolution yield estimation, has clear methodological value. However, I believe several aspects of the manuscript need to be further strengthened to improve its rigor, interpretability, and the practical usability of the resulting data product.

**Reply:** Thank you for your positive feedback and recognition of our work. In the revision, we have carefully addressed your thoughtful comments and suggestions to improve our manuscript.

Specific Comments:

**1.Clarify the use of the term "Label-free".**

The manuscript currently presents "Label-free" as a central contribution, but this term may be somewhat misleading. I suggest that the authors define it more precisely, for example as "field-label-free training," "simulation-driven training," or "simulation-driven yield estimation." This distinction should be clearly stated in the abstract, introduction, and methods sections to avoid the impression that the entire study is completely free of any field observations.

**Reply：** Thank you very much for your insightful and constructive comment. We completely agree with the reviewer that using the absolute term "label-free" without precise contextual boundaries could lead to conceptual confusion, as the Gated Recurrent Unit (GRU) model does rely on the yield outcomes simulated by the WOFOST model as target labels during its training phase.

To eliminate any potential ambiguity and ensure strict terminological rigor, we have thoroughly revised the manuscript. Specifically, we have consistently replaced the term "label-free" with "field-label-free training" throughout the title, abstract, introduction, and Methods section. This revision explicitly clarifies that our framework is completely free of real-world / in situ ground yield annotations during the model training loop.

Specifically, we have added a dedicated statement in the Introduction to clearly define the exact meaning and scope of "field-label-free".

*To address these challenges, this study proposes a field-label-free training framework for maize yield estimation that couples mechanistic model with deep learning.*

*To address the aforementioned challenges, this study constructs a field-label-free training framework for large-scale maize yield estimation.*

*From a practical application perspective, this study not only constructs a low-cost, scalable, mechanism-driven, field-label-free training estimation solution…*

**2.Add comparisons with existing yield products.**

The manuscript would benefit from a more systematic comparison with existing public yield products, such as SPAM and the "A 10 m maize, rice and soybean yield dataset from 2016 to 2021 in Northeast China" dataset. Both visual comparisons and quantitative accuracy assessments would help demonstrate the added value of the proposed product. In addition, the reported accuracy appears to be lower than that of current existing machine-learning-based yield estimation studies. The authors should discuss the possible reasons for this difference, such as the simulation-to-reality gap, limited field observations, simplified management assumptions, or uncertainties in remote-sensing inputs.

**Reply：** Thank you for this constructive comment and for highlighting these two important aspects. We appreciate the opportunity to clarify our comparative evaluation and the underlying sources of yield estimation uncertainty. Below, we address both points in detail:

**1. Comparison with Existing Public Yield Products**

We fully agree that comparing our product with established regional yield datasets enhances the credibility and demonstrates the added value of our map.(Teng et al., 2026)

In the revised manuscript, we have acquired the published *"A 10 m maize, rice and soybean yield dataset from 2016 to 2021 in Northeast China"* dataset. We conducted a systematic quantitative validation and cross-comparison between our product, this public dataset, and official county-level statistical yearbooks for overlapping years.

***3.5.2 Comparison with Existing Public Yield Products***

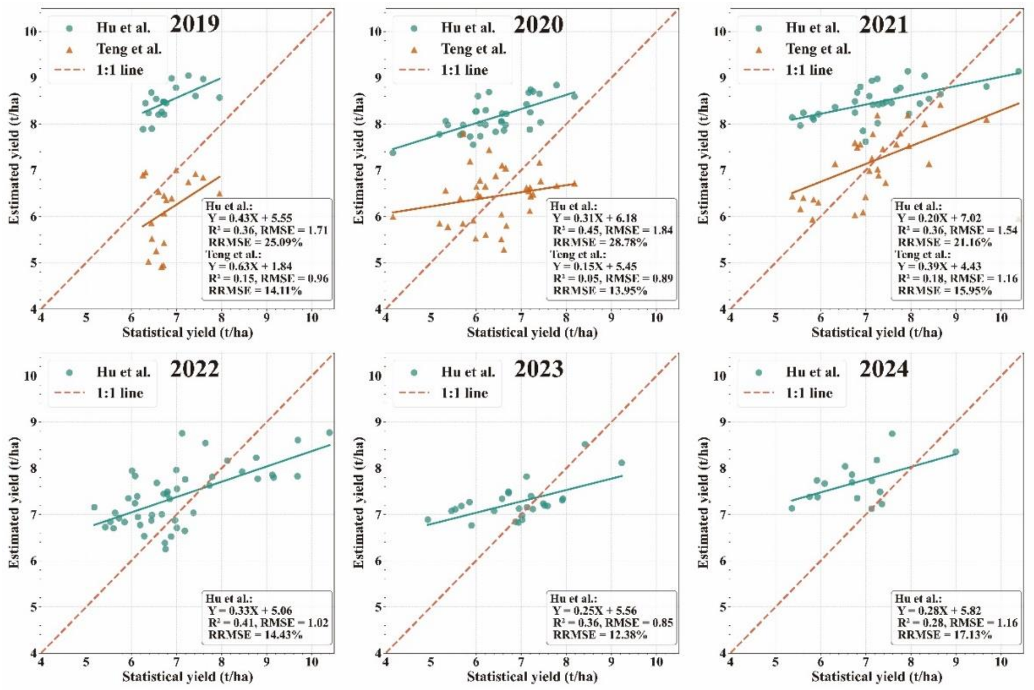


***Figure 14 County-level comparison of maize yield estimates between our product and the existing 10-m benchmark dataset*** *(Teng et al., 2026)* ***against official statistical yearbook data in Northeast China (2019–2021).***

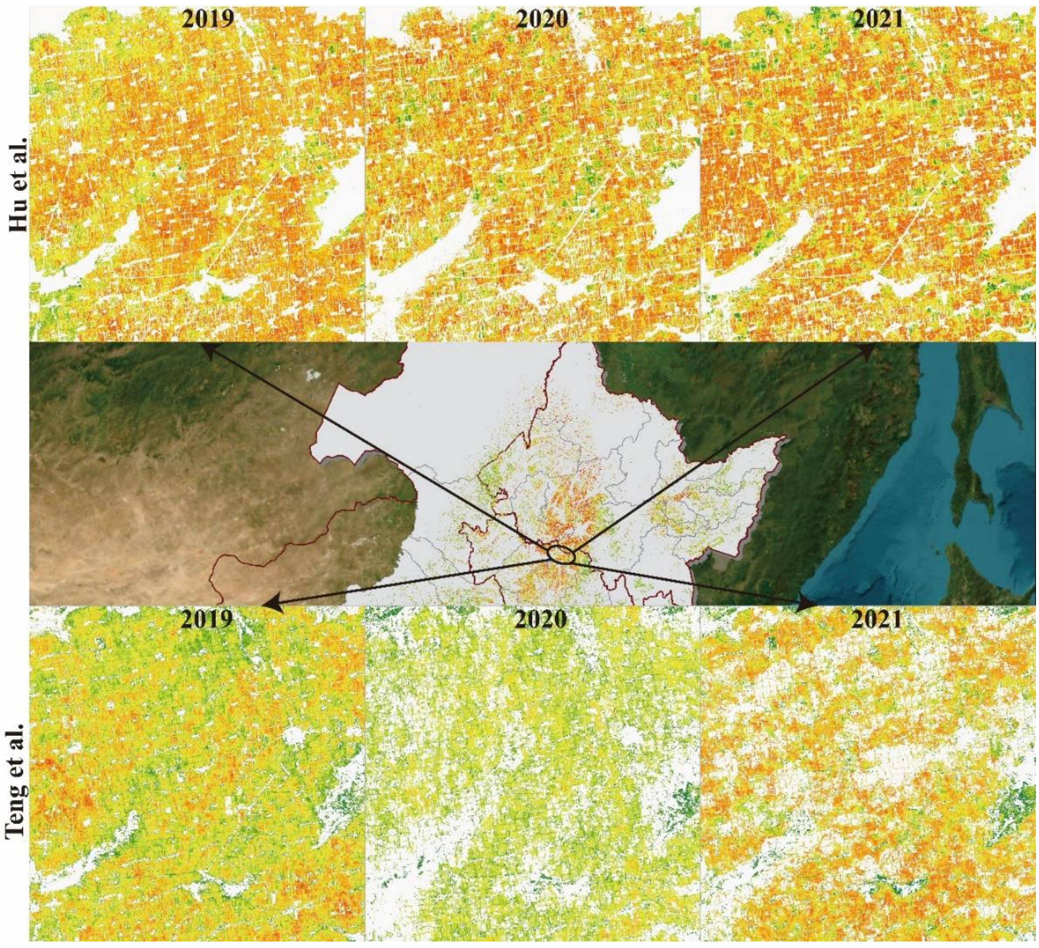

***Figure 15 Visual comparison of spatial maize yield mapping between our product and the existing 10-m benchmark dataset*** (Teng et al., 2026) ***in the major maize-producing areas at the junction of Heilongjiang and Jilin provinces.***

*We compared our product with the publicly available " A 10 m maize, rice and soybean yield dataset from 2016 to 2021 in Northeast China "*(Teng et al., 2026) *over the overlapping period (2019–2021). Both products were evaluated against official county-level statistical yearbook data (Figure 12).*

*As shown in Figure 14, our product achieves consistently higher agreement with county-level statistics across all three years compared to the benchmark dataset. At the county-level (Figure 14), our product demonstrates robust performance across the full 2019–2024 period, with $R^2$ values ranging from 0.28 to 0.45 and RRMSE from 12.38% to 17.13%.*

*Beyond quantitative accuracy, we also assessed the spatial depiction quality of the two products through visual comparison. Figure 15 presents the spatial distribution of estimated maize yields in the major maize-producing area at the junction of Heilongjiang and Jilin provinces. Our product exhibits clearly delineated field boundaries and more spatially continuous within-field patterns, with fewer fragmented or missing pixels. Non-crop linear features such as field ridges are effectively removed, resulting in cleaner and more homogeneous field parcels. Our product achieves favorable accuracy against the existing benchmark and provides added value through extended temporal coverage (2019–2024), improved spatial accuracy at finer administrative scales, and enhanced field-level spatial detail.*

## 2.Possible reasons affecting the accuracy of the report

Regarding the point on reported accuracy, we have dedicated **Section 4.5 (Uncertainties and Limitations)** to thoroughly discuss the primary factors contributing to estimation errors.

### *4.5 Uncertainties and Limitations*

*Although this study achieved relatively high yield estimation accuracy, the model still carries certain uncertainties due to data source limitations and simplified assumptions. The gap between crop growth model simulations and reality, along with input data uncertainties, are the primary sources constraining the reliability of crop yield estimates.*

*The input layer of the WOFOST simulations, including both cultivar parameters and agronomic management settings, inevitably deviates from the complexity of real world conditions. In this study, several key physiological parameters governing phenological development were assigned based on literature values and the model's default settings, rather than calibrated against site-specific field trials for each cultivar. In terms of agronomic management, our framework assumes non-limiting nutrient conditions and discretizes the sowing window into only four fixed dates. In reality, smallholder farmers* *across Northeast China employ flexible sowing schedules and highly diverse management strategies* (Chuanwei et al., 2024). *These two types of input deviations may jointly cause the simulated LAI trajectories to diverge to some extent from actual growth curves in specific fields. Nevertheless, we argue that the full-factorial parameter combination strategy adopted in this study constructs an exhaustive training set that covers a broad physiological and management space. The consistency between estimated yields and statistical yearbook data (Figure 11), together with the robust multi-year independent field validation performance (Section 3.4), demonstrates that the simulated data generated under the current input settings are sufficiently reliable to support accurate yield estimation.*

*A systematic discrepancy also exists between the WOFOST-simulated LAI and the satellite- derived LAI. The simulated values represent a deterministic, noise-free "green leaf area index" at the point scale under idealized atmospheric conditions* (H. et al., 1998). *In contrast, the satellite-retrieved LAI is subject to multiple factors, including residual atmospheric correction errors, cloud-gap filling algorithms, and mixed-pixel effects. As noted by Lu et al.* (2025)*, satellite-derived vegetation parameters (e.g., LAI) are not free from uncertainty, particularly in areas with high LAI or dense canopies, where saturation or underestimation may occur. Moreover, different data processing workflows, such as cloud masking and filtering algorithms, can introduce systematic errors. Consequently, input uncertainties can propagate through the prediction model when a model trained on clean simulated data is generalized to noisy satellite observations* (Xie et al., 2025). *However, the gating mechanism of the GRU provides inherent robustness to such input noise by dynamically weighting the contribution of each time step* (Cho, 2014)*. The stable performance of the model in independent validation across 2022–2024 (Table 7) further confirms that the proposed framework can effectively mitigate the adverse effects of uncertainties in satellite-derived LAI under the current data quality.*

**3.Include additional model-structure comparisons.**

To better justify this model choice, I suggest adding other time-series models, such as LSTM and Transformer-based models, as baseline comparisons. This would help show whether GRU is indeed the most suitable architecture for this task, rather than simply being one possible option.

**Reply：** Thank you for this constructive suggestion. To better justify our architectural

choice and demonstrate the suitability of GRU for this task, we have expanded our baseline comparisons by incorporating the LSTM model under our primary feature configuration (Scheme C).

The quantitative performance comparison between GRU and LSTM has been incorporated into **Section 3.2 (Comparative Performance of Deep Learning Models)**

***3.2.2 LSTM Models***

*As shown in Table 7, the LSTM model achieves moderate performance on the simulation test set ($R^2$ = 0.57, RMSE = 0.96 t/ha) but exhibits substantial degradation when transferred to real-world conditions, with an independent validation $R^2$ of only 0.31 (RMSE = 1.67 t/ha). This substantial gap suggests that GRU's more compact gating mechanism, with fewer parameters, offers superior generalization from simulated training data to noisy real-world satellite observations. Given its competitive performance and higher computational efficienc, GRU was selected as the primary model for this study. The complete LSTM results, including scatter plots of model performance on training, test, and validation sets, along with SHAP feature importance analysis, are provided in* ***Appendix Figure A2***

***Table 7 Performance of LSTM models under Scheme C (Full Features) and independent validation using in situ yield measurements (2022–2024)***

| **Scheme ID** | **Accuracy** | **LSTM model performance on simulation dataset** | | | **Independent validation using measured yield** | | | |
|---|---|---|---|---|---|---|---|---|
| | | Training set | Test set | Validation set | 2022 | 2023 | 2024 | All years combined |
| **C (Full Features)** | $R^2$ | 0.61 | 0.57 | 0.27 | 0.31 | 0.4 | 0.24 | 0.31 |
| | RMSE (t/ha) | 0.91 | 0.96 | 1.25 | 1.77 | 1.52 | 1.84 | 1.67 |
| | RRMSE (%) | 10.06 | 10.6 | 13.85 | 20.65 | 16.82 | 21.22 | 18.99 |

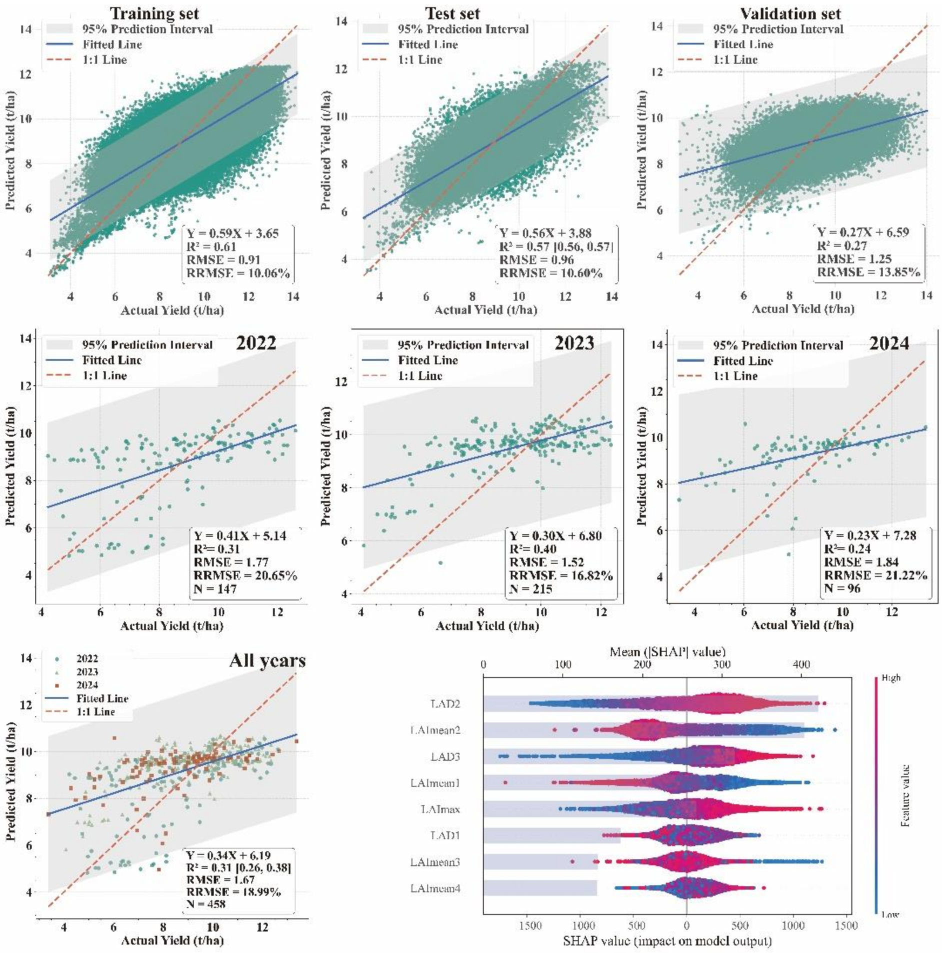

*Figure A2. Performance of LSTM models under Scheme C (Full Features) and independent validation using in situ yield measurements (2022–2024)*

**4.Strengthen the mechanistic interpretability analysis.**

The manuscript mainly relies on feature-combination experiments to assess the effects of different input variables. I think it is not sufficient to support a strong claim of “mechanistic interpretability” .I suggest incorporating model interpretation tools such as SHAP to quantify the dynamic contributions of different factors across growth stages to the final yield estimation. This would provide a clearer understanding of how the model uses information from different phenological periods and environmental variables.

**Reply：** Thank you for this highly valuable and insightful suggestion. In accordance with your recommendation, we have incorporated SHAP (SHapley Additive exPlanations) analysis into our revised manuscript to evaluate feature contributions dynamically. Specifically, we applied SHAP to both our primary GRU model and the newly added LSTM baseline. The complete SHAP interpretability analysis has been incorporated into **Section 3.2.1 (GRU Models)** of the revised manuscript.

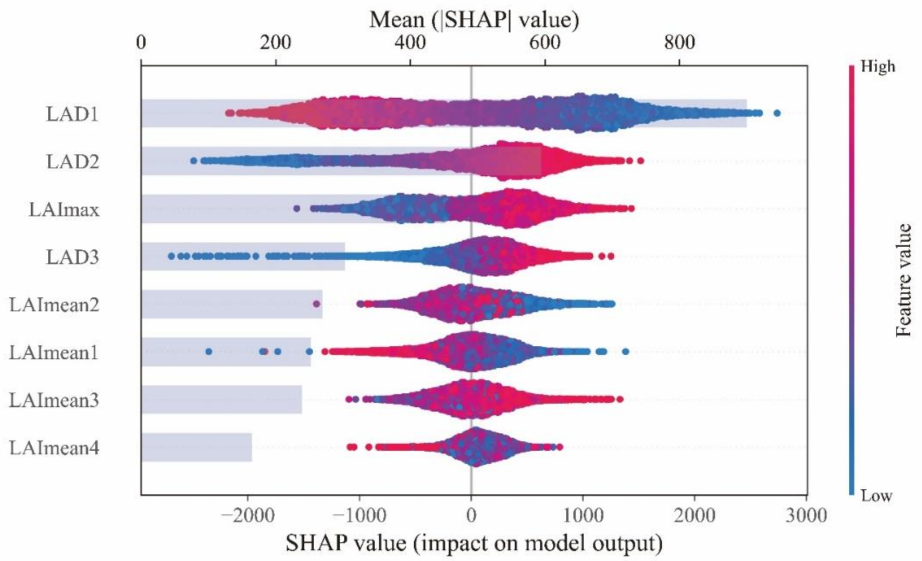


***Figure 7 SHAP feature importance analysis for the optimal GRU model (Scheme C)***

*To provide a quantitative assessment of individual feature contributions, we conducted a SHAP analysis on the optimal GRU model (Scheme C). SHAP provides a unified measure of feature importance by quantifying each input's marginal contribution to the model output across all possible feature subsets. Figure 7 presents the SHAP summary plot for all eight features in Scheme C, with features sorted by their mean absolute SHAP values in descending order. The results reveal that cumulative features ($LAD_1$–$LAD_3$) dominate the model's decision-making, collectively accounting for 56.61% of* *the total SHAP importance. $LAD_1$ (Emergence to Flowering) exhibits the highest individual contribution at 28.35%, followed by $LAD_2$ (Flowering to Milking Maturity) at 18.72% and $LAD_3$ (Milking Maturity to Maturity) at 9.54%. The peak feature $LAI_{max}$ ranks third with 14.25% contribution, indicating that maximum canopy development is an important indicator of yield potential, though secondary to cumulative growth metrics. This implies that achieving a high peak LAI is not sufficient; the temporal accumulation of photosynthetic capacity across the season is more decisive.*

**5.Provide confidence or uncertainty layers for the yield product.**

For a data product intended for practical use, a single yield estimate may not be enough. I suggest providing annual 10 m confidence or uncertainty maps in TIF format. Such layers would allow users to identify where the yield estimates are more reliable and where they should be interpreted with caution.

**Reply：** Thank you for this excellent and practical suggestion. We completely agree that providing spatial confidence or uncertainty layers is crucial for data users to evaluate the reliability of local yield predictions and apply the dataset effectively.

In response to this comment, we have generated annual 10-meter resolution yield uncertainty maps based on Monte Carlo Dropout (MC-Dropout), a widely adopted approach for uncertainty quantification in deep learning models. By performing multiple stochastic forward passes with dropout layers activated during inference, we obtain a distribution of predictions for each pixel, from which we derive the standard deviation and the coefficient of variation (CV = standard deviation / mean). The CV represents the relative prediction uncertainty, providing a normalized metric that facilitates cross-regional comparisons. Due to the intensive computational workload associated with pixel-wise uncertainty quantification across our large-scale study area (approximately $1.24 \times 10^6$ $km^2$) and the current data download and processing constraints of the Google Earth Engine (GEE) platform, we have currently completed and released the uncertainty layers for 2023 and 2024 as a first priority. These two years cover both a normal year (2024) and an extreme flood year (2023), providing users with uncertainty information under contrasting climatic conditions. The remaining historical years (2019–2022) are under active production and will be publicly released as soon as processing completes. We have added a clear description of the uncertainty layer availability in the Data availability section of the revised manuscript. The CV values in the uncertainty layers have been scaled up by a factor of 10,000 for integer storage; users should divide the pixel values by 10,000 to obtain the original CV values.

The detailed description has been incorporated into the revised manuscript in the Data availability section.

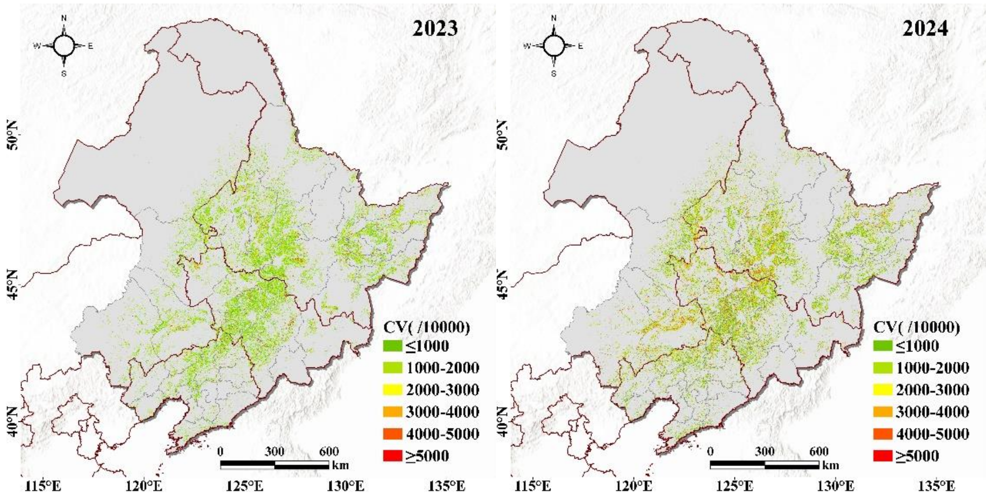


***10-meter resolution uncertainty maps (CV) for 2023 and 2024(True value = pixel value / 10000)***

*The Northeast China Maize Yield 10-m dataset (2019–2024) is openly available at https://zenodo.org/records/19547014 (Hu et al., 2026). Accompanying 10-meter resolution uncertainty layers (coefficient of variation, CV) for 2023 and 2024 are also provided; uncertainty layers for 2019–2022 are under active production and will be released progressively upon completion. The CV layers were generated using Monte Carlo Dropout, with CV values scaled by 10,000 for integer storage; users should divide pixel values by 10,000 to recover the original CV. Users are encouraged to consult these uncertainty layers to assess the spatial reliability of the yield estimates.*

**6.Report uncertainty in model-performance metrics.**

Machine-learning models are affected by randomness in model training, sample splitting, and parameter initialization. Therefore, I suggest reporting uncertainty ranges or confidence intervals for the main accuracy metrics. Methods such as bootstrap resampling, repeated random splits, spatial cross-validation, or Monte Carlo experiments could be used to report the mean and 95% confidence interval of $R^2$, RMSE, MAE, and bias. This would make the performance assessment more robust and more convincing.

**Reply：** We sincerely thank the reviewer for this rigorous and constructive suggestion regarding uncertainty quantification.

We fully agree that reporting uncertainty ranges for model performance metrics is essential for robust assessment, as deep learning models are indeed subject to randomness in training, sample splitting, and parameter initialization.

In response to this comment, we conducted a bootstrap resampling analysis (1,000 iterations with replacement) to quantify the uncertainty of our main accuracy metrics. For the simulation dataset, we repeatedly resampled the test set and computed $R^2$, RMSE, MAE , Bias and RRMSE for all deep learning model configurations (Schemes A–D for GRU, and Scheme C for LSTM), reporting the mean values with their 95% confidence intervals. For the independent field validation, we applied the same bootstrap procedure to the combined 2022–2024 in situ measurements to capture the uncertainty arising from limited sample size and inter-annual variability. The detailed results have been incorporated into the revised manuscript as **Table A2 Bootstrap-derived uncertainty estimates (mean, standard deviation, and 95% confidence intervals) for deep learning model performance metrics** in **Appendix A**

***Table A2 Bootstrap-derived uncertainty estimates (mean, standard deviation, and 95% confidence intervals) for deep learning model performance metrics.***

| Models | Phase | Scheme | Metric | Mean | Std | 2.5% CI | 97.5% CI |
|---|---|---|---|---|---|---|---|
| GRU | Simulation test | A(Mean Features) | $R^2$ | 0.453 | 0.003 | 0.447 | 0.460 |
| | | | RMSE (t/ha) | 1.070 | 3.257 | 1.064 | 1.077 |
| | | | MAE (t/ha) | 0.837 | 2.687 | 0.832 | 0.843 |
| | | | Bias (t/ha) | -0.020 | 0.004 | -0.029 | -0.011 |
| | | | RRMSE (%) | 11.834 | 0.037 | 11.763 | 11.912 |
| | | B(Integral Features) | $R^2$ | 0.307 | 0.003 | 0.300 | 0.314 |
| | | | RMSE (t/ha) | 1.207 | 0.003 | 1.200 | 1.213 |
| | | | MAE (t/ha) | 0.958 | 0.003 | 0.953 | 0.963 |
| | | | Bias (t/ha) | -0.070 | 0.005 | -0.079 | -0.061 |
| | | | RRMSE (%) | 13.379 | 0.038 | 13.304 | 13.451 |
| | | C(Full Features) | $R^2$ | 0.663 | 0.003 | 0.658 | 0.668 |
| | | | RMSE (t/ha) | 0.841 | 0.003 | 0.835 | 0.847 |
| | | | MAE (t/ha) | 0.645 | 0.002 | 0.640 | 0.649 |
| | | | Bias (t/ha) | -0.019 | 0.003 | -0.025 | -0.013 |
| | | | RRMSE (%) | 9.323 | 0.035 | 9.257 | 9.392 |
| | | D(Selected Subset) | $R^2$ | 0.271 | 0.003 | 0.265 | 0.276 |
| | | | RMSE (t/ha) | 1.238 | 0.004 | 1.231 | 1.245 |
| | | | MAE (t/ha) | 0.987 | 0.003 | 0.980 | 0.993 |
| | | | Bias (t/ha) | -0.004 | 0.005 | -0.013 | 0.005 |
| | | | RRMSE (%) | 13.723 | 0.042 | 13.645 | 13.807 |
| | Field Validation | A(Mean Features) | $R^2$ | 0.270 | 0.038 | 0.199 | 0.346 |
| | | | RMSE (t/ha) | 1.895 | 0.074 | 1.752 | 2.046 |
| | | | MAE (t/ha) | 1.458 | 0.058 | 1.348 | 1.578 |
| | | | Bias (t/ha) | -0.432 | 0.085 | -0.598 | -0.264 |
| | | | RRMSE (%) | 21.475 | 0.835 | 19.921 | 23.173 |
| | | B(Integral Features) | $R^2$ | 0.495 | 0.058 | 0.384 | 0.607 |
| | | | RMSE (t/ha) | 2.195 | 0.136 | 1.950 | 2.465 |
| | | | MAE (t/ha) | 1.728 | 0.110 | 1.530 | 1.958 |
| | | | Bias (t/ha) | -0.797 | 0.170 | -1.135 | -0.473 |

| | | | | | | | |
|---|---|---|---|---|---|---|---|
| | | | RRMSE (%) | 25.599 | 1.677 | 22.453 | 28.945 |
| | | C(Full Features) | $R^2$ | 0.689 | 0.021 | 0.649 | 0.728 |
| | | | RMSE (t/ha) | 1.210 | 0.028 | 1.155 | 1.264 |
| | | | MAE (t/ha) | 1.029 | 0.030 | 0.973 | 1.087 |
| | | | Bias (t/ha) | -0.134 | 0.057 | -0.244 | -0.025 |
| | | | RRMSE (%) | 13.710 | 0.345 | 13.043 | 14.384 |
| | | D(Selected Subset) | $R^2$ | 0.308 | 0.037 | 0.239 | 0.384 |
| | | | RMSE (t/ha) | 1.808 | 0.063 | 1.689 | 1.933 |
| | | | MAE (t/ha) | 1.417 | 0.051 | 1.321 | 1.515 |
| | | | Bias (t/ha) | 0.758 | 0.077 | 0.603 | 0.918 |
| | | | RRMSE (%) | 20.490 | 0.840 | 18.899 | 22.176 |
| LSTM | Simulation test | A(Mean Features) | $R^2$ | 0.565 | 0.003 | 0.559 | 0.571 |
| | | | RMSE (t/ha) | 0.955 | 0.003 | 0.949 | 0.962 |
| | | | MAE (t/ha) | 0.740 | 0.003 | 0.735 | 0.745 |
| | | | Bias (t/ha) | -0.047 | 0.004 | -0.054 | -0.039 |
| | | | RRMSE (%) | 10.594 | 0.037 | 10.526 | 10.667 |
| | Field Validation | A(Mean Features) | $R^2$ | 0.314 | 0.030 | 0.255 | 0.375 |
| | | | RMSE (t/ha) | 1.675 | 0.049 | 1.576 | 1.769 |
| | | | MAE (t/ha) | 1.352 | 0.045 | 1.263 | 1.437 |
| | | | Bias (t/ha) | 0.361 | 0.077 | 0.201 | 0.510 |
| | | | RRMSE (%) | 18.987 | 0.661 | 17.671 | 20.277 |

**7.Explain how the model captured typhoon-related flood-induced yield losses in 2023.**

The manuscript highlights the model's ability to capture yield losses caused by typhoon-related flooding in 2023. However, if WOFOST was mainly run under a water-limited mode, the simulated training samples would primarily represent water deficit or drought stress rather than yield losses caused by excessive soil moisture or waterlogging. The authors should explain which input signals allowed the model to detect flood-related yield reductions. Was the decline in LAI the main pathway? Were precipitation anomalies, soil moisture conditions, abrupt vegetation-index changes, or post-disaster canopy recovery also involved? If waterlogging processes were not explicitly represented in the simulations, this limitation should be clearly acknowledged in the discussion.

**Reply：** Thank you for this highly perceptive and insightful comment. We completely agree that clarifying the physiological mechanism and key input signals that enabled the model to capture typhoon-induced flood losses in 2023 is essential for a accurate interpretation of our results.

In accordance with your suggestion, we have added a dedicated analysis in **Section 4.4 (*Simulation and Model Response to Extreme Precipitation Stress*)** to explain the underlying mechanism and explicitly acknowledge the model's inherent limitations:

***4.4 Simulation and Model Response to Extreme Precipitation Stress***

*In this study, the WOFOST model was operated under the water-limited production mode, which is not equivalent to simulating only drought stress. The WOFOST soil water balance module is driven by actual daily precipitation and dynamically tracks changes in daily soil moisture content (van Diepen et al., 1989). Although the WOFOST model does not explicitly simulate the full range of physiological processes associated with anaerobic root conditions under waterlogging, this simplification does not prevent the model from capturing waterlogging-induced yield losses. When cumulative precipitation exceeds the soil drainage and runoff capacity, the model inherently triggers excess-water stress responses—suppressing root oxygen availability, limiting canopy transpiration and photosynthesis, and ultimately reducing LAI and biomass accumulation(H. et al., 1998; Liu et al., 2020). Therefore, our training dataset inherently includes yield reduction scenarios caused by excessive soil moisture, which originate directly from the 30-year historical meteorological records (1995–2024). Sentinel-2 satellite observations are capable of capturing such LAI anomaly signals, and the GRU model has learned, during the training phase, the general mapping relationship between depressed LAI trajectories and reduced final yields under various environmental stresses. When applied to real satellite imagery, the model does not explicitly detect flood events; instead, it infers yield losses through the observed LAI decline as a comprehensive stress signal.*

**8.Expand the range of WOFOST simulation scenarios.**

Although the study generates a series of crop-model simulations, the simulation settings appear to be relatively simplified. For example, soil parameters are limited to four major loam types, and only four fixed sowing dates are considered. These assumptions may not fully capture the diversity of real-world field conditions. The authors should consider adding more combinations of sowing dates, soil parameters, water management, fertilization levels, and irrigation scenarios to improve the representativeness of the simulated training samples.

**Reply：** Thank you for this thoughtful suggestion regarding the expansion of simulation scenarios. We fully agree that the representativeness of simulated training samples is critical for the success of our field-label-free framework, and we appreciate the opportunity to clarify our simulation design rationale.

However, our current simulation settings, while appearing simplified, were deliberately designed to maximize the coverage of physiologically plausible growth trajectories through a full-factorial parameter combination strategy, rather than exhaustively enumerating all possible agronomic combinations, which would be computationally prohibitive and potentially introduce redundant samples.

Firstly, The four loam subclasses selected in our study (coarse-textured sandy loams, light-textured loams, intermediate-textured medium loams, and fine-textured heavy loams) represent the dominant soil texture classes across the Northeast China maize belt, covering over 85% of the cultivated area in the study region (Shi et al., 2004). While we acknowledge that soil heterogeneity exists at finer scales, the WOFOST model's hydrological module is primarily sensitive to soil texture-derived hydraulic parameters (wilting point, field capacity, saturation, and hydraulic conductivity).

Secondly, The four fixed sowing dates (April 20, April 30, May 10, and May 20) were selected to represent the typical range of actual sowing practices across Northeast China. Rather than arbitrarily increasing the number of sowing date scenarios, which would primarily shift the phenological timeline without fundamentally altering the shape of the growth trajectory, our full-factorial design combined these four dates with extensive crop parameter variations (192 crop parameter combinations), ensuring that the training dataset encompasses a wide range of growth rates, phenological durations, and stress responses.

Thirdly, the exhaustive factorial combination of multiple parameters (192 crop parameter combinations, 4 soils, 4 sowing dates, 60 station, 30 years, 3,686,400 valid samples) already ensures that the training dataset covers the vast majority of physiologically plausible growth trajectories under Northeast China's climatic and edaphic conditions. This scale is substantially larger than most previous surrogate modeling studies. Adding more soil subclasses or sowing dates would increase sample size but with diminishing returns in terms of physiological state space coverage.

Fourthly, as stated in Section 2.4.1, maize production in Northeast China is predominantly rainfed, and fertilizer application generally follows standardized regional practices that are not a limiting factor for growth. Therefore, operating the WOFOST model under water-limited mode with non-limiting nutrient assumptions is scientifically appropriate for the study region.

Ultimately, the strong performance of our model in independent field validation ($R^2$ = 0.69, RMSE = 1.21 t/ha) across multiple years provides empirical evidence that the current simulation settings are sufficiently representative to support accurate real-world yield estimation. We believe this outcome serves as the most compelling validation of our simulation design.

We have clarified this rationale in the revised manuscript by expanding the methodological justification in Section 2.4.2, emphasizing that our full-factorial design prioritizes physiological state space coverage over sheer scenario enumeration.

*By systematically combining long-term meteorological records from 60 stations spanning 30 years, four major soil texture types, four representative sowing dates, and extensive crop parameter variations (192 crop parameter combinations), a maize* *growth simulation dataset with pronounced spatiotemporal heterogeneity was constructed using the PCSE framework. Our full-factorial design prioritizes physiological state space coverage over exhaustive enumeration of all possible agronomic combinations, ensuring that the training dataset encompasses a wide range of growth rates, phenological durations, and stress responses under Northeast China's climatic and edaphic conditions. In total, 3,686,400 valid simulation samples were generated, and the detailed parameter combinations are summarized in Table 3. This dataset preserves complete time series trajectories of leaf area index (LAI) under diverse environmental stress conditions, together with the corresponding final grain yield, thereby providing a comprehensive crop growth simulation dataset for subsequent deep learning surrogate model training.*

**9.Add validation at a finer administrative scale.**

Validation based only on prefecture- or city-level yield statistics may be too coarse and could mask local spatial biases. I suggest collecting county-level maize yield statistics for the three northeastern provinces from 2019 to 2024, if available, and using them for additional validation. This would provide a more rigorous assessment of the spatial accuracy of the proposed yield product.

**Reply：** Thank you for your suggestion. We fully agree that city-level aggregation may

obscure local spatial variations and fail to provide a rigorous assessment of spatial accuracy. In response to this comment, we have now acquired official county-level maize yield statistics for the three northeastern provinces for the period 2019–2024 and conducted an additional validation at the county scale. The detailed results have been incorporated into the revised manuscript in **Section 3.5.2 (Comparison with Existing Public Yield Products)**, along with the comparison against the existing 10-m benchmark dataset (Teng et al., 2026) , which provides a more rigorous assessment of the spatial accuracy of our proposed product.

The detailed results are presented in Section 3.5.2 of the revised manuscript, with quantitative county-level validation shown in Figure 14.

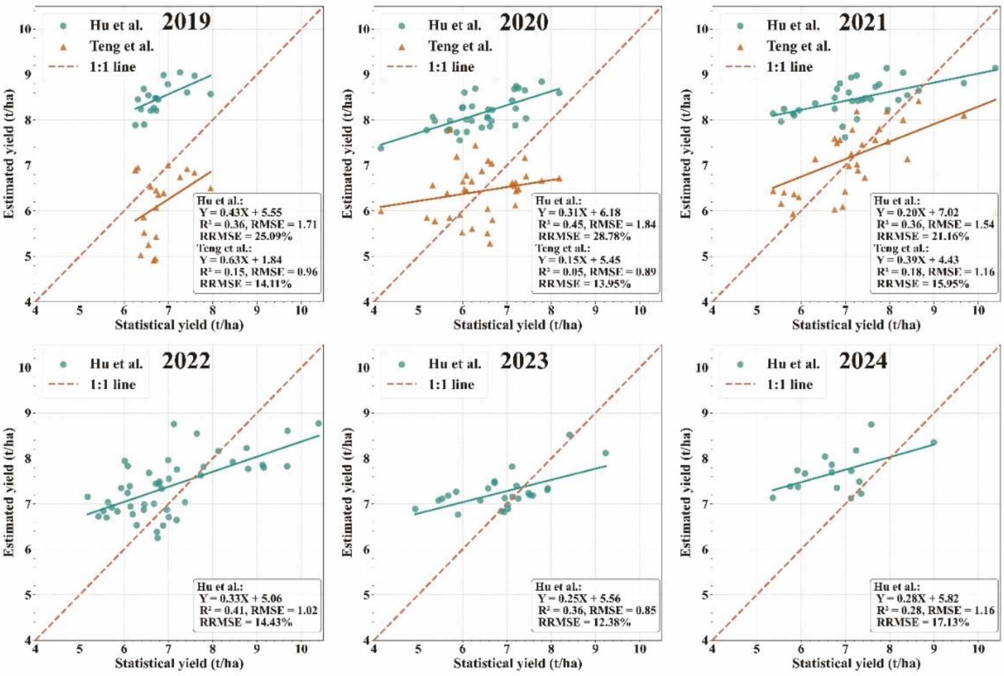


***Figure 14 County-level comparison of maize yield estimates between our product and the existing 10-m benchmark dataset (Teng et al., 2026) against official statistical yearbook data in Northeast China (2019–2021).***

*We compared our product with the publicly available " A 10 m maize, rice and soybean yield dataset from 2016 to 2021 in Northeast China "(Teng et al., 2026) over the overlapping period (2019–2021). Both products were evaluated against official county-level statistical yearbook data (Figure 14).As shown in Figure 14, our product achieves consistently higher agreement with county-level statistics across all three years compared to the benchmark dataset. At the county-level, our product demonstrates robust performance across the full 2019–2024 period, with $R^2$ values ranging from 0.28 to 0.45 and RRMSE from 12.38% to 17.13%.*

**10.Discuss the simulation-to-reality gap more explicitly.**

A key assumption of this study is that a deep-learning model trained on crop-model simulations can be successfully transferred to real remote-sensing conditions. Therefore, the gap between simulated samples and real-world fields is central to the reliability of the method. I suggest adding a dedicated discussion of this simulation-to-reality gap, including uncertainties related to crop-model parameters, management practices, remote-sensing LAI retrieval, meteorological inputs, and the absence or simplification of certain real-world stress processes such as flooding.

We sincerely thank the reviewer for raising this critical issue. We fully agree that the simulation-to-reality gap is central to the reliability of our proposed framework, as the fundamental premise of our approach—training a deep learning model entirely on simulated data and transferring it to real-world satellite observations—depends critically on the representativeness of the WOFOST simulations. In response to this comment, we have added a dedicated and comprehensive discussion to explicitly address this gap. Specifically, we have significantly extended Section 4.5 (Uncertainties and Limitations) to systematically enumerate the key discrepancies between the simulated and real domains.

***4.5 Uncertainties and Limitations***

*Although this study achieved relatively high yield estimation accuracy, the model still carries certain uncertainties due to data source limitations and simplified assumptions. The gap between crop growth model simulations and reality, along with input data uncertainties, are the primary sources constraining the reliability of crop yield estimates.*

*The input layer of the WOFOST simulations, including both cultivar parameters and agronomic management settings, inevitably deviates from the complexity of real world conditions. In this study, several key physiological parameters governing phenological development were assigned based on literature values and the model's default settings, rather than calibrated against site-specific field trials for each cultivar. In terms of agronomic management, our framework assumes non-limiting nutrient conditions and discretizes the sowing window into only four fixed dates. In reality, smallholder farmers across Northeast China employ flexible sowing schedules and highly diverse management strategies (Chuanwei et al., 2024). These two types of input deviations may jointly cause the simulated LAI trajectories to diverge to some extent from actual growth curves in specific fields. Nevertheless, we argue that the full-factorial parameter combination strategy adopted in this study constructs an exhaustive training set that covers a broad physiological and management space. The consistency between estimated yields and statistical yearbook data (Figure 11), together with the robust multi-year independent field validation performance (Section 3.4), demonstrates that the simulated data generated under the current input settings are sufficiently reliable to support accurate yield estimation.*

*A systematic discrepancy also exists between the WOFOST-simulated LAI and the satellite- derived LAI. The simulated values represent a deterministic, noise-free "green leaf area index" at the point scale under idealized atmospheric conditions (H. et al., 1998). In contrast, the satellite-retrieved LAI is subject to multiple factors, including residual atmospheric correction errors, cloud-gap filling algorithms, and mixed-pixel effects. As noted by Lu et al. (2025), satellite-derived vegetation parameters (e.g., LAI) are not free from uncertainty, particularly in areas with high LAI or dense canopies, where saturation or underestimation may occur. Moreover, different data processing workflows, such as cloud masking and filtering algorithms, can introduce systematic errors. Consequently, input uncertainties can propagate through the prediction model when a model trained on clean simulated data is generalized to noisy satellite observations (Xie et al., 2025). However, the gating mechanism of the GRU provides* *inherent robustness to such input noise by dynamically weighting the contribution of each time step (Cho, 2014). The stable performance of the model in independent validation across 2022–2024 (Table 7) further confirms that the proposed framework can effectively mitigate the adverse effects of uncertainties in satellite-derived LAI under the current data quality.*


Cho, K.: Learning phrase representations using RNN encoder-decoder for statistical machine translation, arXiv preprint arXiv:1406.1078, 2014.

Chuanwei, Z., Gao, J., Liu, L., and Wu, S.: Simulating the effects of optimizing sowing date and variety shift on maize production at finer scale in northeast China under future climate, Journal of the Science of Food and Agriculture, 104, https://doi.org/10.1002/jsfa.13247, 2024.

van Diepen, C. a., Wolf, J., van Keulen, H., and Rappoldt, C.: WOFOST: A simulation model of crop production, Soil Use Manage., 5, 16–24, https://doi.org/10.1111/j.1475-2743.1989.tb00755.x, 1989.

H., B., Diepen, C. A., Rötter, R. P., and HH, van: WOFOST7.1: A user's guide, https://doi.org/10.13140/RG.2.1.1814.1282, 1998.

Hu, J., Du, X., Li, Q., Zhang, Y., Wang, H., Luo, J., Xu, J., Zhao, Y., Zhang, Z., Dong, Y., and Shen, Y.: NortheastChinaMaizeYield10m: A 10-m resolution maize yield dataset for northeast China (2019–2024) generated via a mechanistically interpretable, label-free framework, , https://doi.org/10.5281/zenodo.19547014, 2026.

Liu, K., Harrison, M., Shabala, S., Meinke, H., Ahmed, I., Zhang, Y., Tian, X., and Zhou, M.: The state of the art in modeling waterlogging impacts on plants: What do we know and what do we need to know, Earth's Future, https://doi.org/10.1029/2020EF001801, 2020.

Lu, J., Li, J., Fu, H., Zou, W., Kang, J., Yu, H., and Lin, X.: Estimation of rice yield using multi-source remote sensing data combined with crop growth model and deep learning algorithm, Agric. For. Meteorol., 370, 110600, https://doi.org/10.1016/j.agrformet.2025.110600, 2025.

Teng, F., Wang, M., Shi, W., Pan, L., Guo, J., and Xiao, X.: A 10 m maize, rice and soybean yield dataset from 2016 to 2021 in northeast China, Sci Data, 13, 344, https://doi.org/10.1038/s41597-026-06719-0, 2026.

Xie, J., Zhang, D., Jin, N., Cheng, T., Zhao, G., Han, D., Niu, Z., and Li, W.: Coupling crop growth models and machine learning for scalable winter wheat yield estimation across major wheat regions in China, Agric. For. Meteorol., 372, 110687, https://doi.org/10.1016/j.agrformet.2025.110687, 2025.